

LETTER TO THE EDITOR

Ultrahigh-density silicon nanobridges formed between two vertical silicon surfaces

M Saif Islam, S Sharma, T I Kamins and R Stanley Williams

Quantum Science Research, Hewlett-Packard Laboratories, 1501 Page Mill Road, MS 1123, Palo Alto, CA 94304, USA

E-mail: saif@hpl.hp.com

Received 15 September 2003

Published 23 January 2004

Online at stacks.iop.org/Nano/15/L5 (DOI: 10.1088/0957-4484/15/5/L01)

Abstract

We report simultaneous lateral growth of a high density of highly oriented, metal-catalyzed silicon nanowires on a patterned silicon substrate and bridging of nanowires between two vertical silicon sidewalls, which can be developed into electrodes of an electronic device. After angled deposition of catalytic metal nanoparticles on one of two opposing vertical silicon surfaces, we used a metal-catalyzed chemical vapour deposition process to grow nanowires and eventually form mechanically robust ‘nanobridges’. The growth and bridging of these nanowire arrays can be integrated with existing silicon processes. This method of connecting multiple nanowires between two electrodes offers the high surface-to-volume ratio needed for nanosensor applications.

1. Introduction

Free-standing nanostructures are currently being extensively explored [1–4]. They are especially attractive for sensor applications because their high surface-to-volume ratio makes them very sensitive to charged species adsorbed on their surfaces. Lateral growth of carbon nanotubes between two electrodes during chemical vapour deposition (CVD) has been reported [5]; a lateral electric field applied between the electrodes attracts the growing nanotube towards the counter-electrode. Although the potential of carbon nanotubes for applications such as gas-sensing field-effect devices has been demonstrated [6], the difficulty of synthesizing only metallic or only semiconducting nanotubes and the difficulty of modifying nanotube surfaces have limited their development as nanosensors [7]. Lateral growth of GaAs nanowhiskers by metalorganic vapour phase epitaxy (MOVPE) from vertical ridges on a GaAs substrate using Au nanoparticles as the catalyst has also been demonstrated [8, 9]. However, the properties of the mechanical connection between a bridging nanowire and the vertical sidewall have not been reported.

Nanowires made of silicon are especially attractive because of silicon’s compatibility with existing IC processes. Moreover, the chemical and physical properties of Si can be controlled to adjust the device sensitivity, and Si nanowires can be selectively grown. Using Si allows the vast knowledge of Si technology to be applied to applications such as sensing.

Using semiconductor nanowires, researchers have demonstrated electrical sensors for biological and chemical species [7], and designed a range of nanoelectronic and photonic devices in different material systems [10, 11]. In many of these demonstrations, nanowires were assembled after growth into parallel or crossed arrays by alignment aided by fluid flow [12] or by applying electric fields [10]. In other cases, electrical contacts were defined with electron-beam lithography on a few selected nanowires [11]. Although connecting electrodes to nanowires one at a time contributes to understanding the characteristics of nanowires and exploring novel device applications, it cannot be used for reproducible mass-fabrication of dense, low-cost device arrays. A massively parallel, self-assembly technique is needed to allow ‘bridging’ of Si nanowires between electrodes using only relatively coarse lithography, and combining assembly with the nanowire growth is attractive.

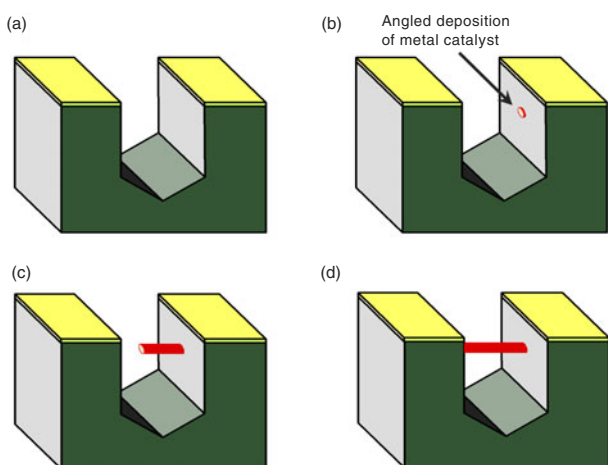


Figure 1. Schematic diagrams of (a) trench formation, (b) catalyst deposition, (c) lateral nanowire growth, and (d) bridging across trench.

In this letter, we report the lateral growth of highly oriented, metal-catalyzed Si nanowires from vertical Si planes using two different catalysts and connection of the nanowires to other vertical Si planes during growth; the Si adjacent to the vertical planes can be further developed into electrodes. By using large numbers of such ‘nanobridges’ in parallel, the desired high surface area can be obtained in a small volume.

We and many others [13–15] have previously demonstrated that semiconductor nanowires often grow nearly normal to the surface of a (111)-oriented Si wafer and make good electrical [15] and mechanical connection to the substrate. If (111) surfaces can be oriented vertically, the nanowires should grow laterally. (110)-oriented Si wafers contain vertical (111) planes, and anisotropic wet chemical etching of a masked (110)-oriented Si wafer in KOH can etch a trench into the Si, leaving vertical (111) planes as the sidewalls of the trench [16, 17], as shown schematically in figure 1(a). Nanowires should grow laterally from one sidewall toward the opposing sidewall of the trench (figure 1(c)). If the two vertical surfaces bounding the trench are closely spaced, the laterally growing nanowires should impinge on the opposing vertical surface, as shown schematically in figure 1(d). If a connection can form during the nanowire growth (i.e., by self-assembly), the nanowires become increasingly attractive for sensors and other device applications requiring electrical conduction. We will show that the nanowires make robust mechanical connection when they impinge on the opposing sidewall.

2. Experimental technique

Ti- and Au-nucleated Si nanowires are used in the experiments reported here. A thermal oxide layer was first grown on (110)-oriented Si wafers, and patterned to serve as an etch mask for the subsequent Si etch. The mask edges were carefully aligned along the intersections of vertical (111) planes with the top surface so that the subsequently etched trench is bounded by two (111) surfaces. The oxide was etched using reactive ion etching (RIE) with CHF_3 and Ar gases, and the Si was etched in 44% KOH– H_2O at 110 °C for 1 min to create trenches approximately 8 μm deep and 2–15 μm wide. Figure 2(a)

shows an etched Si(110) wafer with exposed Si(111) vertical planes bounding the trenches.

After forming the vertical (111) surfaces and cleaning the samples, the nucleating metal catalyst—Ti or Au of the order of 1 nm thick—was deposited by electron-beam evaporation onto the vertical (111) surfaces of the etched grooves. The samples were held at an angle of 45° from the normal to deposit the catalyst on only one sidewall of the trench so that the wires would grow preferentially from one sidewall in this demonstration. (This one-sided growth is not critical for the bridged structure, but allowed the nucleating and impinging ends of the nanowires to be studied separately.) Because of the geometry of the structure and deposition angle, no catalyst was deposited on the bottoms of trenches narrower than 8 μm . Catalyst was deposited on the bottoms of wider trenches and also on the masking oxide on the top surface between trenches.

The samples were then transferred through air to a lamp-heated CVD reactor, in which the samples are supported by an SiC-coated graphite plate of moderate thermal mass. They were annealed in hydrogen at ~625 °C to form Au–Si alloy nanoparticles and to reduce the native oxide on the Ti and form TiSi_2 . The temperature was then increased to ~635 °C, and a mixture of SiH_4 and HCl was introduced into the hydrogen ambient to grow the nanowires. The total pressure was controlled at 10 Torr, with 3 slm of hydrogen, 15 sccm of SiH_4 , and 15 sccm of HCl. The nanowires were grown for 30 min.

After nanowire deposition, the samples were examined by plan-view scanning electron microscopy (SEM) and cleaved for study by cross-sectional SEM.

3. Results and discussion

We previously demonstrated the synthesis of Si nanowires using Ti-catalyzed growth [1], and others have reported Au-catalyzed Si nanowires [14] grown by CVD. Briefly, in this technique, the Si adatoms resulting from decomposition of an Si-containing gas diffuse through or around a TiSi_2 or Au–Si nanoparticle and precipitate on the underlying substrate. The continued precipitation at the nanoparticle–Si interface causes the nanoparticle to remain at the tip of an epitaxially growing column of Si of similar diameter. Figure 2(b) illustrates Au-nucleated Si nanowires growing laterally from one (111)-oriented trench face toward the opposing face. The 8 μm -long nanowires extend only partially across the 15 μm -wide trench shown in figure 2(b). The longest nanowires are 10 μm long, while >90% have a length of $\sim 8 \pm 0.7 \mu\text{m}$. Typical nanowires have a diameter of $180 \pm 20 \text{ nm}$. For gaps 8 μm wide or less, many Au-nucleated nanowires extend completely across the trench, as shown for an 8 μm -wide trench in figure 2(c). Most Au-nucleated nanowires are straight, and ~70% of them intersect the opposing sidewall at an angle of $90^\circ \pm 0.5^\circ$. Figure 2(d) shows a Ti-nucleated Si nanowire bridging a 2.5 μm -wide trench. The diameter of the nanowire is 200 nm near its base, and 150 nm near its impinging end.

The connection between the Si sidewall and the impinging nanowire is critical to the use of the bridging structure. In the case of Au-nucleated Si nanowires, the nanowire carries a molten droplet of Au–Si alloy at its tip. As the nanowire impinges on the opposing sidewall, the axial growth stops, and the molten alloy spreads radially, contributing to catalytic

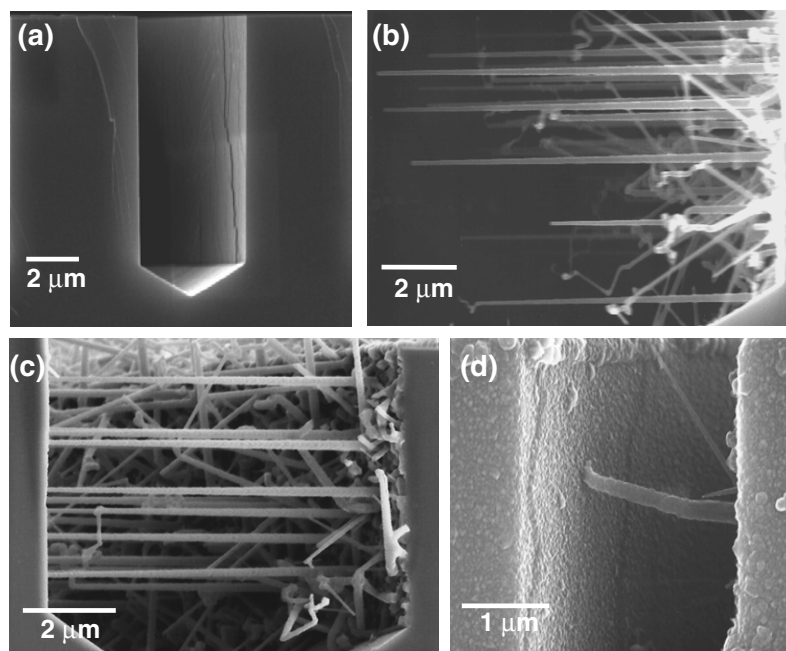


Figure 2. Cross-section scanning electron micrographs (SEMs) of (a) a 4 μm -wide, anisotropically etched trench in a Si(110) wafer; (b) Au-catalyzed, lateral epitaxial nanowire growth from a (111) sidewall surface into a 15 μm -wide trench; (c) Au-catalyzed, lateral epitaxial nanowire growth across an 8 μm -wide trench, connecting to opposing sidewall. (d) Ti-catalyzed lateral growth of a Si nanowire to form a bridge across a 2.5 μm -wide trench. The direction of nanowire growth is from the right to the left in (b)–(d).

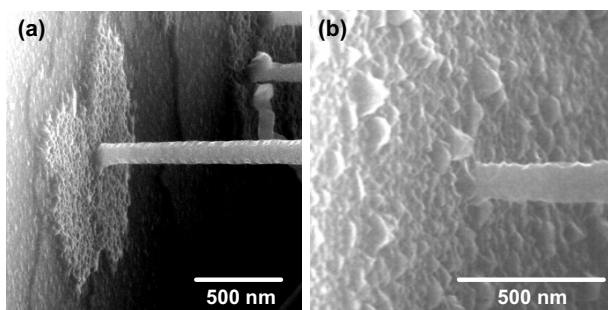


Figure 3. (a) Detail of a disc formed along the (111) sidewall surrounding the impinging end of an Au-nucleated nanowire. (b) Detail of the impinging end of a Ti-nucleated Si nanowire making a rigid connection with the opposing sidewall.

decomposition of SiH_4 and further accelerated deposition. This continued accelerated deposition forms a disc of material extending radially outward from the contact point along the (111) Si sidewall of the trench, as shown in figure 3(a). The disc is often thicker near its edges, showing the importance of lateral diffusion (either along the surface of the sidewall or in the gas phase) in supplying SiH_4 to the disc. The size of the disc at the impinging end continues to increase with additional time after the nanowire bridges the trench. Consequently, the diameter and thickness of the disc are greater for narrower trenches because of the longer time after nanowire bridging, as plotted in figures 4(a) and (b), which show the diameter and thickness of the disc for trenches of varying width. The disc diameter varies from approximately 600 nm to 2 μm , and its thickness varies from 10 to 70 nm. In the case of Ti-nucleated nanowires, however, the catalyzing TiSi_2 nanoparticle at the tip of the growing nanowire remains in the solid state. Thus,

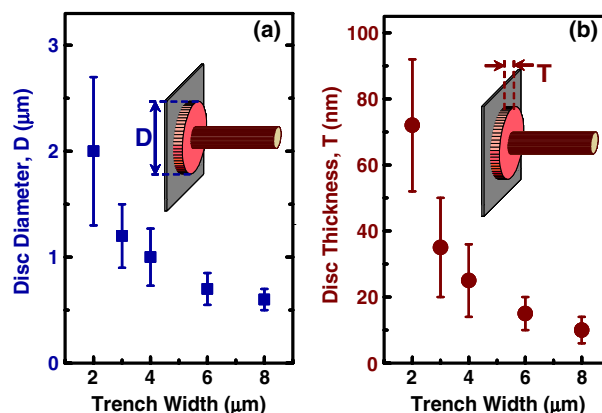


Figure 4. (a) Diameter and (b) thickness of discs extending from impinging nanowires along the sidewalls of trenches after bridging as a function of trench width.

the nature of the connection of the impinging nanowire to the opposing sidewall is expected to be different than for the Au-nucleated nanowires. A connection is formed after a Ti-nucleated Si nanowire impinges on the opposing sidewall, as shown in figure 3(b). However, we did not observe a disc-like deposit surrounding the nanowire at the impinging end, unlike the case of Au-nucleated nanowires, probably because of the lower diffusivity of the catalyst in the solid phase than in the liquid phase.

For application of these nanowires in devices, the connection between the sidewall and the impinging nanowire must be mechanically strong. The structures shown in figures 5(a) and (b) indicate the robustness of the connection. Several of the nanowires have broken, probably during cleaving for SEM examination. Au- and Ti-nucleated

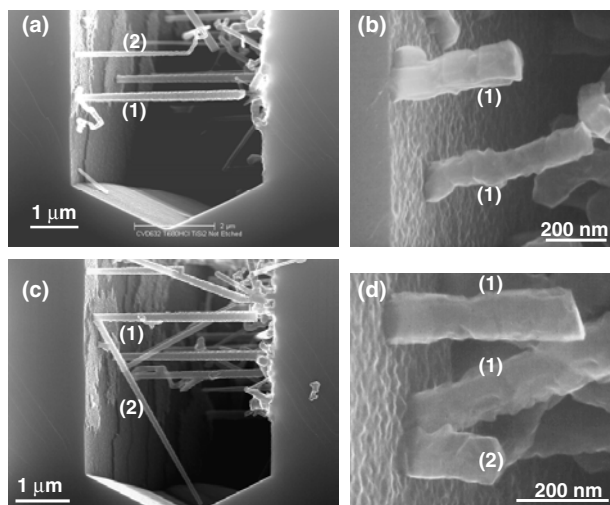


Figure 5. (a) An Au-nucleated bridging nanowire (labelled 1) broken so that the impinging end is still supported at the opposing sidewall. (b) Ti-nucleated Si nanowires forming a rigid connection at the impinging end, as shown by the broken nanowires supported at the opposing sidewall. In (a) and (b) the direction of growth of the nanowires is from the right to the left. (c) Secondary nanowire growth from the disc region formed at the impinging end of an Au-nucleated, bridging Si nanowire (labelled 2). (d) Secondary nucleation at the impinging end of a Ti-nucleated bridging nanowire.

nanowires shown in figures 5(a) and (b), respectively, are broken such that the initially grown base section of the nanowire has been removed and the section of the wire grown later remains and is supported by the connection of the impinging end of the nanowire to the sidewall. Having the nanowire break in the middle, rather than at the end, indicates that the connection at the impinging end of the nanowire is mechanically strong, as it is at the base end.

For effective bridging, the nanowires must have adequate mechanical rigidity to grow without elastic deformation and must not be deflected by the flow of gas in the CVD reactor or when they impinge on the opposing Si(111) crystal face. When used as sensors, they must not be deformed by the flow of the gas or liquid they are measuring. Thus, nanowires with somewhat larger diameters are advantageous.

Since the tips of the growing nanowires contain significant amounts of Au or Ti, catalyst is transported across the trench by the nanowires. During extended deposition after the nanowires impinge on the opposing sidewall, the transported catalyst can lead to additional nucleation of nanowires. Figures 5(c) and (d) show secondary nanowire growth near the impinging ends of Au- and Ti-nucleated nanowires, respectively. This secondary nucleation from the (111) plane adjacent to the impinging end of a nanowire is more prevalent in narrower trenches (e.g., $<4 \mu\text{m}$ for Au-nucleated nanowires), where the deposition continues for an extended period after the nanowires impinge on the opposing sidewall, thus promoting secondary nanowire nucleation. With the deposition parameters of the present experiment, we observed secondary nucleation in more than 25% of the Au-nucleated bridging nanowires grown in trenches narrower than $4 \mu\text{m}$.

With continued growth, the secondary nanowires can reach the other sidewall of the trench and eventually cause

tertiary nucleation, which we observed occasionally in $2 \mu\text{m}$ -wide trenches. Although an average length of $8 \mu\text{m}$ was observed for the straight Au-nucleated nanowires, the average total length of nanowires with secondary and tertiary nucleation was $6.5 \mu\text{m}$ (including the lengths of the primary, secondary and tertiary nanowires). The shorter length of this type of nanowire suggests some delay before secondary and tertiary nucleation events occur.

4. Conclusion

We have demonstrated the growth of laterally oriented, metal-catalyzed Si nanowires bridging between vertical (111) Si planes formed by anisotropically etching a (110)-oriented Si wafer. The bridges are mechanically robust and resist considerable force. More work is needed to understand the mechanical sensitivity to gravity, mechanical vibration and acceleration, and liquid and gas flow.

By employing only optical lithography, a large array of nanoscale sensors can be fabricated between biasing electrodes. The electrically isolated electrodes can be formed by using a highly doped semiconductor layer on top of an insulator, such as a silicon-on-insulator structure. This nanowire structure combines the advantages of 'bottom up' fabrication of nanostructures with 'top down' formation of the connecting electrodes using only coarse optical lithography. It offers an approach for the fabrication of nanoscale electronic devices that avoids costly and slow electron-beam lithography. Nanobridges constructed by the method described in this letter may provide some of the vital building blocks needed to enable the emerging technology of nanoelectronics.

This work was partially supported by DARPA under Agreement MDA972-01-3-0005. The authors thank Xuema Li for expert experimental assistance.

References

- [1] Kamins T I, Williams R Stanley, Basile D P, Hesjedal T and Harris J S 2000 *J. Appl. Phys.* **89** 1008
- [2] Morales A M and Lieber C M 1998 *Science* **279** 208
- [3] Zhu H W, Xu C L, Wu D H, Wei B Q, Vajtai R and Ajayan P M 2002 *Science* **296** 884
- [4] Vigolo B, Pénicaud A, Coulon C, Sauder C, Pailler R, Journet C, Bernier P and Poulin P 2000 *Science* **290** 1331
- [5] Fan S, Chapline M G, Franklin N R, Tomblor T W, Cassell A M and Dai H 1999 *Science* **283** 512
- [6] Kong J, Franklin N R, Zhou C, Chapline M G, Peng S, Cho K and Dai H 2000 *Science* **287** 622
- [7] Cui Y, Wei Q, Park H and Lieber C M 2001 *Science* **293** 1289
- [8] Haraguchi K, Hiruma K, Katsuyama T, Tominaga K, Shirai M and Shimada T 1996 *Appl. Phys. Lett.* **69** 386
- [9] Haraguchi K, Hiruma K, Hosomi K, Shirai M and Katsuyama T 1997 *J. Vac. Sci. Technol. B* **15** 1685
- [10] Duan X, Huang Y, Cui Y, Wang J and Lieber C M 2001 *Nature* **409** 66
- [11] Chung S-W, Yu J-Y and Heath J R 2000 *Appl. Phys. Lett.* **76** 2068
- [12] Huang Y, Duan X, Wei Q and Lieber C M 2001 *Science* **291** 630
- [13] Kamins T I and Williams R Stanley 2003 *mstnews* **3/03** 12
- [14] Westwater J, Gosain D P, Tomiya S, Usui S and Ruda H 1997 *J. Vac. Sci. Technol. B* **15** 554
- [15] Tang Q, Liu X, Kamins T I, Solomon G S and Harris J S Jr 2002 *Materials Research Society Fall Mtg. (Boston, MA, Dec. 2002)* (Paper F6.9)
- [16] Kendall D L 1979 *Annu. Rev. Mater. Sci.* **9** 373
- [17] Allen D M and Routledge I A 1983 *IEE Proc. I* **130** 49